



Contents lists available at ScienceDirect

## Computational Materials Science

journal homepage: [www.elsevier.com/locate/commatsci](http://www.elsevier.com/locate/commatsci)

## Comments on “Atomistic modeling of an Fe system with a small concentration of C”

R.G.A. Veiga<sup>a,b</sup>, C.S. Becquart<sup>c,\*</sup>, M. Perez<sup>a</sup><sup>a</sup> Université de Lyon, INSA Lyon, MATEIS, UMR CNRS 5510, 25 Avenue Capelle, F69621 Villeurbanne, France<sup>b</sup> Departamento de Engenharia Metalúrgica e de Materiais, Escola Politécnica da Universidade de São Paulo, Av. Professor Mello de Morais, 2463 Butantã, São Paulo, SP, Brazil<sup>c</sup> Unité Matériaux et Transformations (UMET), Ecole Nationale Supérieure de Chimie de Lille, UMR CNRS 8207, Bat. C6, F59655 Villeneuve d'Ascq Cedex, France

## ARTICLE INFO

## Article history:

Received 11 July 2013

Received in revised form 19 September 2013

Accepted 22 September 2013

Available online 18 October 2013

## Keywords:

FeC alloys

Interatomic potential

Molecular dynamics

## ABSTRACT

The iron–carbon EAM potential that we have developed [Comput. Mater. Sci. 40 (2007) 119] was found to predict a saddle point slightly off the tetrahedral position. This problem was fixed by adding a Gaussian function to the Fe–C pairwise function, which does not change neither the position corresponding to the local energy minimum, i.e. the octahedral site, nor the energy of the saddle point. The potential energy landscape around the saddle point is now more realistic, without changing the dynamics properties of the former potential.

© 2013 Elsevier B.V. All rights reserved.

An iron–carbon EAM potential has been developed by Becquart, Raulot and co-workers [1]. It was fitted to *ab initio* calculations for a carbon atom in dilute solid solution occupying either an octahedral or a tetrahedral site in a cubic simulation box with 128 iron atoms arranged on a bcc lattice. The Fe–Fe interactions are described by the interatomic potential developed by Ackland and Mendelev [2], which provides a good description (compared to both *ab initio* calculations and experiments) of many bulk properties and is currently considered to be the state-of-the-art potential for  $\alpha$ -iron [3]. Despite the fact that this Fe–C potential was fitted to the data corresponding to only two simple configurations (i.e., an isolated carbon atom sitting on an octahedral or a tetrahedral site), its application to other configurations (e.g., two carbon atoms in neighboring positions) have been seen to compare well with *ab initio* calculations or experiments, as one can see in Table 5 in Ref. [1]. This potential has been successfully used in a number of works recently published [4–8].

In order to accurately model carbon diffusion in the bcc iron matrix, a good description of the migration path is required. C atoms in bcc Fe are situated on octahedral positions (noted O). An octahedral position, in turn, is located in the center between a pair of Fe atoms that are second nearest neighbors. According to the orientation of the Fe pairs, one can distinguish three octahedral variants ([100], [010], or [001]). A carbon atom occupying an O-site migrates to an adjacent O-site through a tetrahedral site

(noted T) in the middle of the path. Tetrahedral variants can also be discerned considering the orientation of the pair of O-sites. For instance, a carbon atom occupying an [100] O-site can jump either to a [010] or to a [001] O-site (there are two of each). In the first case, the initial and the final O-sites are aligned in the [001] direction; therefore the T-site between them is labelled a [001] T-variant. The same reasoning can be applied to find the [100] and [010] tetrahedral variants.

A number of interatomic potentials were derived to model Fe–C systems. An older Fe–C potential by Ruda et al. [9], for instance, returns accurate mechanical properties but yields the tetrahedral site more favorable energetically compared to the octahedral site, in contradiction with what is currently accepted. Considering the more recent Fe–C potential developed by Hepburn and Ackland [10], in turn, the octahedral site is the energy minimum for an interstitial carbon in bcc iron, but the tetrahedral position is not the energy maximum along the carbon migration path [11]. For the time being, our Fe–C potential is, to our knowledge, one of the potentials that better describes the minimum energy path for carbon migration in bcc iron. However, it was found recently [12] that our Fe–C potential provides a poor description of the potential energy landscape in the vicinity of the tetrahedral site. The aim of this communication is to underline the needs for patching the original Becquart–Raulot potential [1] and to provide the reader with all necessary information to reconstruct the patched potential.

In Ref. [1], the tetrahedral site is said to correspond to the saddle point for carbon migration in bulk  $\alpha$ -Fe according to the

\* Corresponding author. Tel./fax: +33 3 20 43 49 44.

E-mail address: [charlotte.becquart@univ-lille1.fr](mailto:charlotte.becquart@univ-lille1.fr) (C.S. Becquart).

**Table 1**

Parameters of the cross Fe–C potential.

$i$	$a_i$ (eV/Å <sup>3</sup> )	$b_i$ (Å)
1	25.8403449446387	1.57392207030071
2	5.29633693622809	2.50697533078414
3	4.03000262768764	2.55706258348374
4	−7.23257363478654	2.74993431502404
5	−7.91809159848018	3.11129997684853
6	0.283612435794859	3.50162017458081
7	12.1869023019844	1.64805018491946
8	9.19127905165634	3.08003832563079

**Table 2**

Parameters of the C electron density potential a.u. means density arbitrary units.

$i$	$c_i$ (a.u./Å <sup>3</sup> )	$d_i$ (Å)
1	−16.205911	0.5
2	−0.245035	4.54378

**Table 3**

Parameters used in the C embedding function potential a.u. means density arbitrary units.

F1 (eV a.u. <sup>−0.5</sup> )	−2.78333808071882
F2 (eV a.u. <sup>−2</sup> )	$1.45647907575885 \times 10^{-3}$

EAM potential. The migration energy, which is the difference of the total energies of the carbon atom sitting on the tetrahedral and the octahedral sites, is 0.85 eV. However, some simulations performed in the frame of Veiga PhD work [12] for testing purposes reached a different conclusion. These simulations were as follows. First, a cubic simulation box with 16,000 iron atoms ( $20 \times 20 \times 20$  unit cells) was built. Then, a number of planes perpendicular to the migration path followed by a carbon atom from a [100] O-site to a [001] O-site, passing through a [010] T-site, was defined. This corresponds to an octahedral-to-octahedral path along the [010] direction. For every plane, a rectangle of area  $0.1 \times 0.1$  nm<sup>2</sup> with the octahedral-to-octahedral line passing through its center was divided into a uniform grid (grid spacing of 0.005 nm).

Molecular statics simulations were performed using LAMMPS [13]. A carbon atom was inserted in a position corresponding to a grid point. The carbon atom was kept fixed at its position while the iron atoms were allowed to fully relax, except Fe atoms situated at a distance less than 0.15 nm from the 6 box faces. The latest condition ensured that the whole box did not move in order to get the C atom back at the octahedral site. To prevent spurious interactions between the carbon atom and the fixed Fe atoms, the distance between the interstitial atom and the rigid walls was larger than 2 nm.

Fig. 1 shows the energy contour maps for each plane. Each point in the maps represents the total energy of the system with a carbon

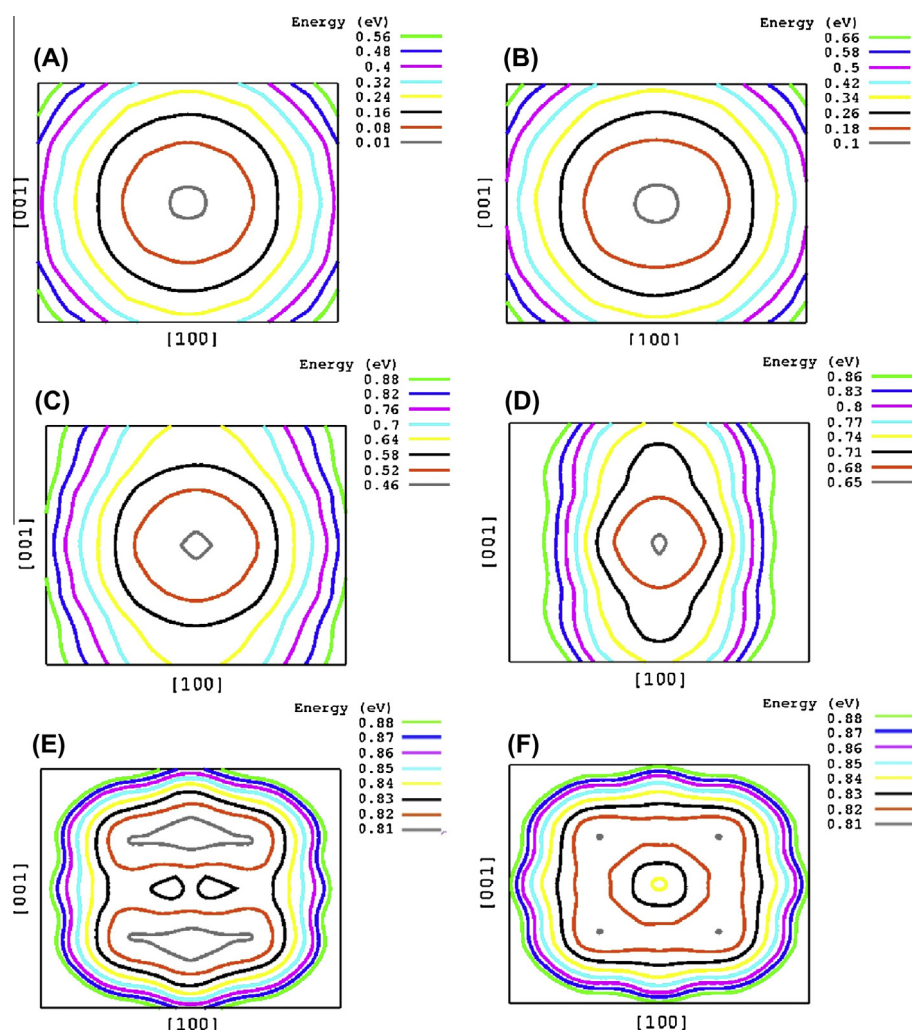


**Fig. 1.** Energy mapping on several planes perpendicular to a [010] carbon migration path: (A) origin (plane containing the O-site), (B) origin + 0.02 nm, (C) origin + 0.05 nm, (D) origin + 0.06 nm, (E) origin + 0.07 nm, (F) origin + 0.07138 nm (plane containing the T-site).

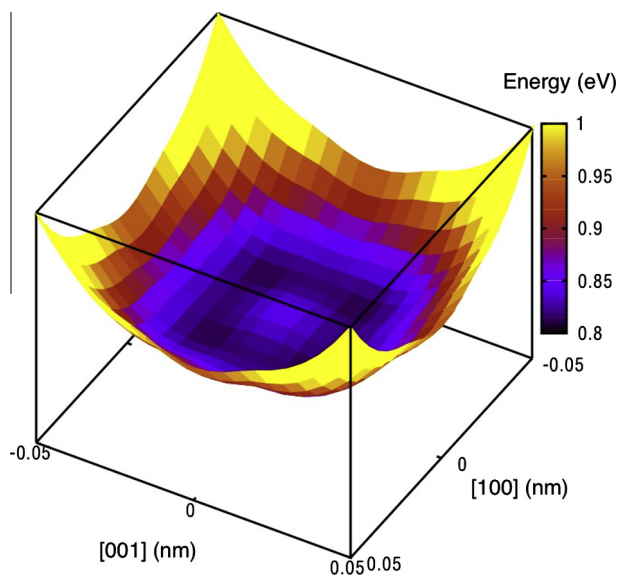


**Fig. 2.** Energy mapping on the plane perpendicular to the [010] direction that contains the tetrahedral site (in the center) obtained by the original Fe–C EAM potential. The energy reference is the total energy of the simulation box with the carbon atom occupying the octahedral site.

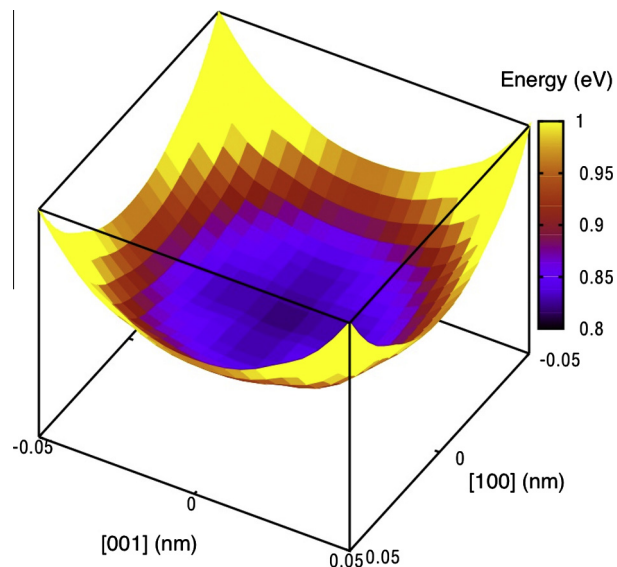


**Fig. 3.** Energy mapping on the plane perpendicular to the [010] direction that contains the tetrahedral site (in the center) obtained by the modified Fe–C EAM potential. The energy reference is the total energy of the simulation box with the carbon atom occupying the octahedral site.

atom at that position minus the total energy of the carbon atom in the octahedral site. We can see in this sequence of maps that the minimum energy path is unique – the minimum of each plane is found right in its center – up to very close to the tetrahedral site, where the minimum energy path is split into four degenerate saddle points, yielding an energy barrier of 0.81 eV. Therefore, the actual energy barrier for carbon migration predicted by the original EAM potential is 0.04 eV lower than the energy barrier reported in [1]. The positions of the saddle points were  $T_x \pm 0.015$  nm,  $T_z \pm 0.015$  nm where  $T_x$  is the  $x$  coordinate of the T-site (along the [100] direction) and  $T_z$  is its  $z$  coordinate (along the [001] direction). From these simulations, the conclusion that one can reach is that the T-site, according to the Fe–C potential, is a local

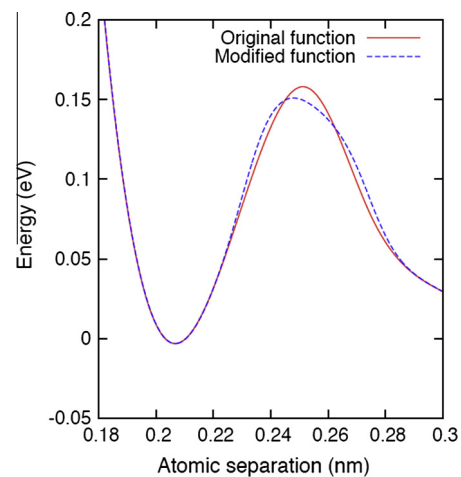


**Fig. 4.** Fe–C pair component of the original potential compared to the modified potential.

maximum on the plane, not a minimum, as it must be if it were the saddle point.

The solution for this problem was not trivial. We first identified that when the system is at one of the four energy minima on the plane that contains the tetrahedral site, represented in Fig. 1(E), the carbon atom does not have four iron atoms at a distance of 0.257 nm as second nearest neighbors. It has two second nearest neighbors at a distance of 0.236 nm and two, now third, nearest neighbours at a distance of 0.271 nm. Our attempts consisted of adding Gaussian functions to the Fe–C pairwise interaction function  $\phi(r)$  near  $r = 0.257$  nm in order to lower the second derivative at this point. A set of three Gaussian functions  $g(r) = \sum a_i \exp[-(r - r_i)^2 / 60\sigma]$  were added and brought the saddle point back to the tetrahedral site. The parameters of the Gaussian functions are  $a_1 = -0.01$ ,  $a_2 = a_3 = 0.01$ ,  $r_1 = 0.2539$  nm,  $r_2 = 0.2365$  nm,  $r_3 = 0.2713$  nm, and  $\sigma = 0.0002$ . In Figs. 2 and 3, one can see the energy mapping on the plane perpendicular to the [010] direction that contains the tetrahedral site (in the center), obtained by molecular statics simulations in the same way as the results shown in Fig. 1 with the original and the modified Fe–C EAM potential, respectively. It can be clearly seen that the modification introduced in the Fe–C potential brings the saddle point back to the tetrahedral site. This modification is obviously very localized as can be seen in Fig. 4 compares the two functions. Consequently, it does change neither the geometry nor the total energy of the local energy minimum, which remains corresponding to the carbon atom in the octahedral site. The activation barrier, obtained by doing MD simulations at different temperatures with one C atom migrating in Fe, has changed by 0.04 eV: it is 0.81 eV with the modified potential, as compared to 0.85 eV [1]. In addition, the configurations in Table 5 in Ref. [1] were simulated with the modified Fe–C potential, and all numbers remained unchanged.

This potential<sup>1</sup> was used with success to model the effect of the stress field of an edge dislocation on carbon diffusion [14], the formation of carbon Cottrell atmospheres in bcc iron [15] as well as the elastic constants of the martensite [16].

## Acknowledgments

This work has been performed within the European PERFECT project (FIGO-CT-2003-508840) and has been partially financed by the European Commission FP7 project PERFORM-60, under

<sup>1</sup> The LAMMPS files for the modified potential can be found at <http://michel.peretz.net.free.fr> and <http://www.ctcms.nist.gov/~cbecker/>

Grant Agreement No. 232612. This work is also a part of the research program of the EDF-CNRS joint laboratory EV2VM (Study and Modelling of the Microstructure for Ageing of Materials). The CAPES/COFECUB project PH 770 13 is also acknowledged. R.G.A. Veiga gratefully acknowledges funding provided by the FAPESP Grant No. 2011/19564-6.

## Appendix A

The potentials were built according to the Embedded-Atom Method. In this scheme, the total energy  $E_{tot}$  of a collection of atoms is given by

$$E_{tot} = \frac{1}{2} \sum_{ij} \Phi_{ij}(r_{ij}) + \sum_i F_i \left( \sum_{j \neq i} \rho_j(r_{ij}) \right)$$

where  $\Phi_{ij}(r_{ij})$  is the pair-interaction energy between atoms  $i$  and  $j$  separated by the distance  $r_{ij}$ ,  $F_i$  is the embedding energy of the atom  $i$  and  $\bar{\rho}_i = \sum_{j \neq i} \rho_j(r_{ij})$  is the host electron density induced by the surrounding atoms  $j$  at the location of the atom  $i$ . The electron-density function assigned to atom  $j$  is  $\rho_j(r_{ij})$ . The pair interaction, electron-density and embedding functions depend on the atoms type. The functions characterizing the pure-Fe potential  $\Phi_{FeFe}(r)$ ,  $\rho_{Fe}(r)$ ,  $F_{Fe}(\bar{\rho})$  are the ones from the original paper ([2]), and Ref. [1] provided the description of the other potential functions ( $\rho_C(r)$ ,  $F_C(\bar{\rho})$ ,  $\Phi_{FeC}(r)$ ). As some errors were uncovered in the parameters published in [1], we provide in this appendix the correct parameterisation (see Tables 1, 2 and 3).

### A.1. Cross Fe–C potential

$$\Phi_{FeC}(r) = \sum_{i=1}^n a_i H(b_i - r)(b_i - r)^3 \quad 1 \leq r \leq 3.502 \text{ \AA}$$

### A.2. C electron density

$$\rho(r) = c_1 H(d_1 - r) + c_2 H(d_2 - r) H(r - d_1)(d_2 - r)^3$$

$$0 \text{ \AA} \leq r \leq 4.808 \text{ \AA}$$

### A.3. Embedding function

$$F(\rho) = F_1 \sqrt{\rho} + F_2 \rho^2$$

$$0 \leq \rho \leq 120$$

## References

- [1] C.S. Becquart, J.M. Raulot, G. Bencteux, C. Domain, M. Perez, S. Garruchet, H. Nguyen, Comput. Mater. Sci. 40 (2007) 119.
- [2] M.I. Mendelev, S. Han, D.J. Srolovitz, G.J. Ackland, D.Y. Sun, M. Asta, Philos. Mag. 83 (2003) 3977; G.J. Ackland, M.I. Mendelev, D.J. Srolovitz, S. Han, A.V. Barashev, J. Phys.: Cond. Mater. 16 (2004) S2629.
- [3] L. Malerba, M.C. Marinica, N. Anento, C. Bjorkas, H. Nguyen, C. Domain, F. Djurabekova, P. Olsson, K. Nordlund, A. Serra, D. Terentyev, F. Willaime, C.S. Becquart, J. Nucl. Mater. 406 (2010) 19.
- [4] E. Clouet, S. Garruchet, H. Nguyen, M. Perez, C.S. Becquart, Acta Mater. 56 (2008) 3450.
- [5] S. Garruchet, M. Perez, Comp. Mat. Sci. 43 (2008) 286.
- [6] Y. Hanlumuayang, P.A. Gordon, T. Neeraj, D.C. Chrzan, Acta Mater. 58 (2010) 5481.
- [7] C.W. Sinclair, M. Perez, R.G.A. Veiga, A. Weck, Phys. Rev. B 81 (2010) 224204.
- [8] R.G.A. Veiga, M. Perez, C.S. Becquart, C. Domain, S. Garruchet, Phys. Rev. B 82 (2010) 054103.
- [9] M. Ruda, D. Farkas, J. Abriata, Scr. Mater. 46 (2002) 349.
- [10] D. Hepburn, G.J. Ackland, Phys. Rev. B 78 (2008) 165115.
- [11] D. Terentyev, N. Anento, A. Serra, V. Jansson, H. Khater, G. Bonny, J. Nucl. Mater. 408 (2011) 272.
- [12] R.G.A. Veiga, PhD dissertation, INSA de Lyon, 2011.
- [13] <http://lammmps.sandia.gov>.
- [14] R.G.A. Veiga, M. Perez, C.S. Becquart, E. Clouet, Acta Mater. 59 (2011) 6963.
- [15] R.G.A. Veiga, J. Phys.: Condens. Matter 25 (2013) 025401.
- [16] N. Gunkelmann, H. Ledbetter, H.M. Urbassek, Acta Mater. 60 (2012) 4901.